Available online at www.sciencedirect.com
ScienceDirect
Journal of Electroanalytical Chemistry 599 (2007) 260–266
Journal of Electroanalytical Chemistry
www.elsevier.com/locate/jelechem

Photoelectrochemistry of 4H–SiC in KOH solutions

D.H. van Dorp *, J.J. Kelly

Condensed Matter and Interfaces, Debye Institute, University of Utrecht, Princetonplein 1, 3508 TA (Utrecht), The Netherlands

Received 23 December 2005; received in revised form 1 March 2006; accepted 6 March 2006
Available online 19 April 2006

Abstract

The photoelectrochemical oxidation of n-type 4H–SiC in KOH solution shows surprising features. While a limiting anodic photocurrent is observed at low light intensity, the semiconductor passivates at high intensity. The photocurrent corresponding to the passivation peak increases linearly with photon flux but decreases when mass transport in the system is enhanced. Characteristic current oscillations are observed. Possible reasons for these results are considered, as is the use of photoanodic etching for practical applications.
© 2006 Elsevier B.V. All rights reserved.

Keywords: SiC; Photoelectrochemistry; KOH; Oscillations; Etching

1. Introduction

Because of its large bandgap, high breakdown electric field and high saturated drift velocity the compound semiconductor silicon carbide is important for device applications under rather extreme conditions [1]. With a lattice constant and thermal expansion coefficient close to those of GaN, SiC is also an attractive substrate for group III nitride-based optoelectronic devices, such as blue light-emitting diodes and diode lasers [2]. Furthermore, extensive work is under way to apply porous SiC in biomedical technology, such as protein dialysis and bone tissue engineering, and in fuel cell technology [3–5].

Etching is an essential step in device fabrication. Dry etching techniques based on reactive ion, electron cyclotron and inductively coupled plasma are used for fabricating (opto)electronic devices. These methods are relatively expensive and may introduce damage in the wafer. In many applications, wet-chemical etching is an attractive alternative [6]. However, the stability of SiC, which results from its covalency combined with a large bandgap and low-lying valence band edge, poses a problem for open-circuit etching. Hole injection into the valence band from stable oxidizing agents in solution is not possible, thus precluding electroless etching. In the case of an n-type semiconductor, photoanodic etching offers a solution. A potential is applied to the semiconductor to create a depletion layer which separates electrons and holes produced by illumination. Holes migrating to the surface cause oxidation and dissolution of the solid [6].

Shor and coworkers have carried out an extensive study of the photoelectrochemistry of SiC (β-SiC, 6H–SiC) in acidic fluoride solution [7–9]. The p-type material could be etched anodically in the dark [9]. Photoanodic dissolution was observed for n-type material [10]. As in the case of Si [11,12], a mesoporous matrix could be formed by electrochemical etching [7]. Anodic etching was also used for patterning with the aid of photolithographic techniques and high etch rates were reported [8]. The need for HF to prevent passivation in acidic electrolyte solutions may be considered a disadvantage for practical applications.

Because of its importance in the technology of microelectromechanical systems (MEMS), anisotropic etching and anodic passivation of Si in alkaline solution have been widely studied [13–15]. Surprizingly, little work has been done on the electrochemistry of SiC at high pH.

* Corresponding author. Tel.: +31 030 2532207; fax: +31 030 2532403.
E-mail addresses: D.H.vanDorp@phys.uu.nl, vandorp@phys.uu.nl (D.H. van Dorp).

0022-0728/$ - see front matter © 2006 Elsevier B.V. All rights reserved.
doi:10.1016/j.jelechem.2006.03.002

Defect-selective etching has been shown for 4H and 6H–SiC [16–18]. Kato et al. describe etching of n-type 6H–SiC under galvanostatic conditions with and without illumination [16]. They report results on the etch rate and surface morphology as a function of current density and KOH concentration. They did not consider the electrochemistry of the system.

In the present work, we have studied the electrochemistry of n-type 4H–SiC in KOH solution. We show that photoanodic oxidation can give high etch rates while at positive electrode potentials passivation, similar to that of Si, is observed. The kinetics of the electrochemical reactions are considered and compared with those of Si in similar solutions. Suggestions are provided for a reaction mechanism. The implications for device etching are considered.

2. Experimental

Single crystal 4H–SiC wafers (0001) were obtained from Umicore, Belgium. The wafers were nitrogen-doped (n-type) and had a resistivity in the range 0.01–0.05 Ω cm. The micro pipe density was $<50\ cm^{-2}$. All samples used in this study had a Si polar face. Ohmic contacts to the SiC were made by evaporating a Ti layer, 100 nm thick, without any additional heat treatment. The SiC sample was glued on a glass substrate and a platinum wire was subsequently connected to the metal contact using a silver epoxy paste. The contact, the sample edges and the platinum wire were isolated from the electrolyte with an Apiezon wax. Unless otherwise stated a vertical electrode geometry was used in a non-stirred solution. For certain experiments a rotating disk electrode (RDE) was used.

Electrochemical measurements were performed in a three-electrode cell with a platinum counter electrode and a saturated calomel electrode (SCE) as a reference. The measurements were performed at 25 °C, unless otherwise stated. All potentials are given with respect to SCE. A potentiostat (EG&G Princeton Applied Research, PAR-273-A) computer-controlled by LabVIEW was used to measure the current-potential curves in the dark and under illumination. Each voltammogram was recorded three times and, unless otherwise stated, the third voltammogram is shown. The light source used was a 500 W Hg arc-lamp (Spectra Physics 66901) with a power supply (Spectra Physics 669910). UV light from the beam was focussed on the sample using a dichroic mirror (280–400 nm) in combination with a plano convex lens. Prior to focussing, the light beam was passed through a water filter. The light intensity was varied with neutral density (ND) filters and in some cases an extra bandpass (BP) filter was used. Before the measurement, the samples were rinsed with acetone.

Electrolyte solutions (0.05–0.5 M) were prepared from a p.a. quality KOH (Merck #105033) and deionised water (Millipore, 18 MΩ cm). The etch experiments were performed for 30 min in 0.1 M KOH solution on a 2×2 mm sample, the rest of the surface was masked with a Teflon sticker. The etched depth was determined with a surface profiler (Alpha-Step 500) and the surface morphology was characterized with a scanning electron microscope (Philips XL 30 SFEG operated at 20 keV), an atomic force microscope (Digital Instruments Nanoscope IIIa) and an optical microscope (Zeiss Axioplan 2).

3. Results

Fig. 1 shows current density–potential plots (j–U) as a function of the light intensity (Φ_{ph}), measured at a constant scan rate of 50 mV/s towards positive potential in 0.1 M KOH solution. For these measurements, the Hg lamp was operated at low intensity; the BP filter was used to reduce the overall output power. In the dark (0% curve) diode characteristics are observed. At negative potential ($U < -1.0$ V) a cathodic current is observed, due to the reduction of water by conduction band electrons. This observation suggests that the flat-band potential is located at value somewhat negative of this potential. The flat-band potential of 6H–SiC under similar conditions is −1.5 V [19]. On illumination, electron-hole pairs are generated. Near the flat-band potential the electric field in the space charge layer is not sufficiently strong to separate the charge carriers. Consequently, the electrons and holes recombine in the bulk and at the surface; no significant increase in current is observed. From −1.0 to +0.50 V the band bending becomes stronger with increasing potential, resulting in a decrease in electron-hole recombination and an increase in current. At potentials above +0.50 V the current levels off to an almost constant value. In the inset of Fig. 1, the current density at +1.0 V is plotted against the light intensity. The current density increase with light intensity is

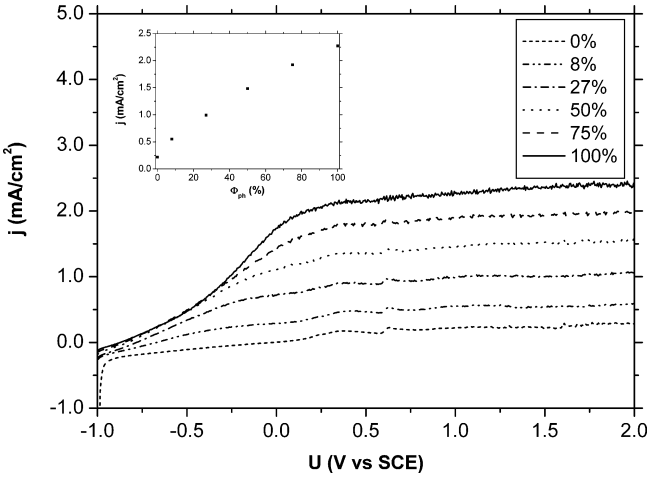

Fig. 1. Current density–potential plots at different light intensities for 4H SiC in 0.1 M KOH solution. The inset shows the current density as function of the light intensity at +1.0 V. The light source was operated at low intensity.

close to linear, suggesting that the hole flux at the surface determines the photocurrent.

In Fig. 2, current density–potential plots are shown for a 0.1 M KOH solution at higher light intensities. A constant scan rate of 25 mV/s towards positive potential was used. For these measurements the Hg lamp operated at full intensity. Several trends can be noted. For the different light intensities a peak in the current is observed, which becomes more pronounced as the light intensity increases. The peak potential is in all cases located at around +0.55 V. The photocurrent at full light intensity at the peak potential measures about 25 mA/cm^2. After the peak potential the current drops quickly and becomes essentially constant. Such current-potential characteristics are typical for passivation of a semiconductor, such as Si whose oxide is partly soluble in the electrolyte solution [20]. In contrast, voltammetric measurements on n-type 6H–SiC in HF solutions do not show such passivation characteristics; the current density instead reaches a limiting value [9]. This implies that the oxide is more soluble in HF solution than in KOH solution. A considerable hysteresis is observed in the photocurrent. When the potential is scanned towards positive values, passivation is observed. When the scan direction is reversed the current drops and then recovers somewhat, indicating a partial removal of the oxide by chemical dissolution. It takes approximately 95 s to remove the oxide completely. Similar measurements were performed in 0.3 and 0.5 M KOH. As expected, the oxide was removed faster in solutions with higher KOH concentration; 23 and 12 s for 0.3 and 0.5 M KOH, respectively. At low KOH concentration (0.05 M), removal of the oxide from the surface was not effective. In addition to the concentration dependence on OH^-, the oxide etch-back time depends on the passivation duration, i.e., the time spent in the passive range during the forward scan. For example at a scan rate of 10 mV/s and a passivation duration of 50 s, the oxide is removed in 150 s. When the passivation duration is decreased to 10 s an oxide etch back time of 80 s is observed.

The inset of Fig. 2 shows that at the peak potential the photocurrent density (j_p) increases linearly with light intensity over the whole intensity range. In the passive range, the photocurrent density shows only a weak dependence on the light intensity.

To investigate a possible influence of oxygen on the surface reactions, the electrolyte solution was deaerated by argon bubbling. This had no effect on the results reported above.

When the temperature of the experiment was raised the passive current increased significantly. The peak current density also showed an increase with temperature, although less drastic; it increased to 42 mA/cm^2 at 71 °C. At this temperature, the passive current became comparable to the peak current.

The influence of the scan rate on the current-potential characteristics is shown in Fig. 3. The measurements were performed in 0.1 M KOH solution close to maximum light intensity. At scan rates higher than 25 mV/s partial removal of the oxide is not observed. Clearly, a certain time is needed for the oxide dissolution. Another feature in Fig. 3 is the shift of the passivation potential towards positive values with increasing scan rate. In a fast scan the oxide has less time to form and therefore passivation of the surface occurs at a later stage in the voltammogram.

Characteristic oscillations in the current were observed at constant potential in the range between the peak potential and the potential at which the surface is fully passivated, as shown in Fig. 4. Voltammograms are included to indicate the position of the potential. The measurements were performed in 0.1 M KOH solution and the voltammograms were recorded at 25 mV/s. The solid line of Fig. 4A shows a current–time plot recorded at 0.5 V, which is at the

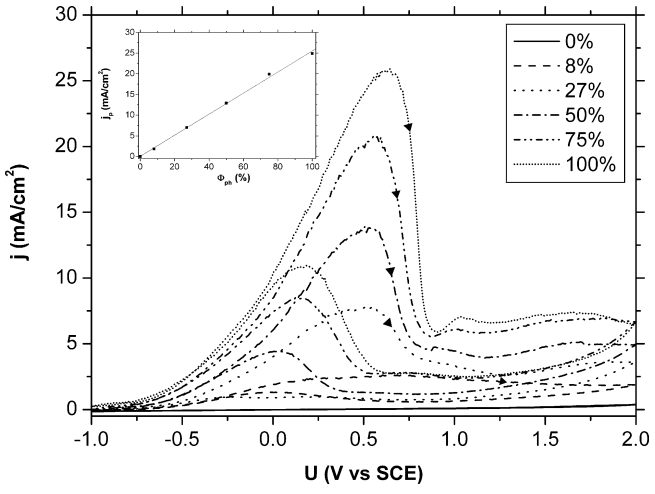

Fig. 2. Current density–potential plots at different light intensities for 4H SiC in 0.1 M KOH solution. The inset shows the photocurrent at the peak (j_p) as a function of the light intensity. The light source was operated at full intensity.

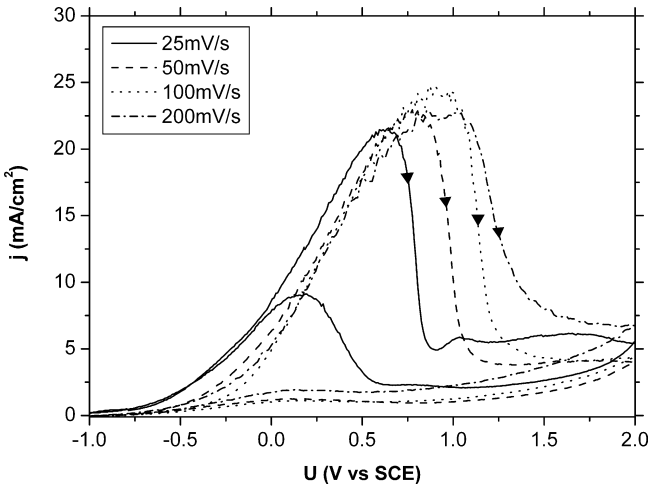

Fig. 3. Influence of the potential scan rate on the *j–U* characteristics for 4H SiC in 0.1 M KOH solution.

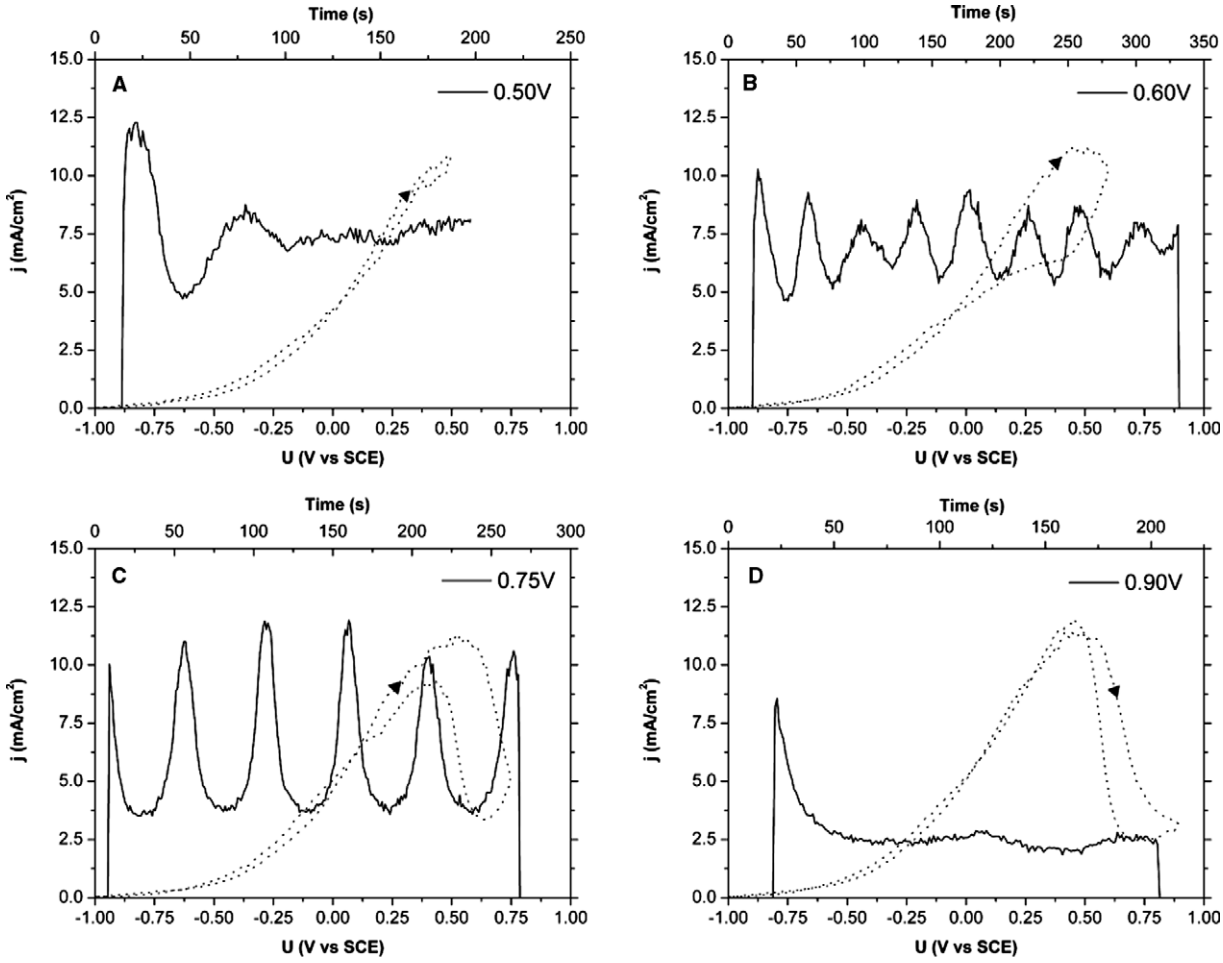

Fig. 4. Current transients at various potentials for 4H–SiC in 0.1 M KOH solution (solid line). The dotted lines show the corresponding voltammograms.

passivation potential. Directly after illumination the current increases quickly to a maximum value. Subsequently, a damped oscillation is observed and the photocurrent goes to a more or less constant value. It should be noted that this damped oscillation was not observed at more negative potentials. When the potential is set to above the peak potential at 0.6 V, the oscillations become more pronounced (Fig. 4(B)) and are not damped. The oscillations are not stable, as indicated by the total charge under each peak, which varies between 228 and 312 mC/cm^2. In contrast, stable and sustained oscillations in the photocurrent are obtained when the potential is further increased to 0.75 V (Fig. 4(C)). In this case, the area under each peak corresponds to 305 ± 3 mC/cm^2. The period of each oscillation is ~51 s. Even after 30 min the oscillations are still well defined. When the potential is further increased to 0.9 V (Fig. 4(D)) the surface becomes passivated, as is clear from the current-potential curve. In this range no oscillations are observed. The transition from oscillation to passivation is very subtle. About 10 mV below the potential at which the surface is fully passivated, the period of the oscillations started to increase and finally a potential difference of 1 mV determined the transition. These measurements clearly indicate that the oscillations are linked to oxide formation and are "killed" when the oxide coverage becomes too high and the surface passivates. This is supported by the observation of current oscillations in the passive range of the voltammograms measured at higher temperature, i.e., at higher oxide etch rates. Oscillations in potential have been reported for galvanostatic etching of 6H–SiC in aqueous KOH solutions [16], suggesting that they are independent of crystal polytype.

Fig. 5 shows the effect of stirring on the current oscillations recorded in 0.1 M KOH solution at 0.7 V. The period increases from 30 s (unstirred solution) to 55 s (stirred solution). In addition, the total charge under the peaks increases from 160 to 210 mC. A shift of the minima and maxima of the curves towards lower current density is also observed. Fig. 5 suggests that improved hydrodynamics may favour passivation; the passive period between two current peaks is increased when the solution is stirred. This rather surprising result is confirmed in cyclic voltammetric measurements with a rotating disk electrode (Fig. 6).

While the general form of the photocurrent-potential curve is not changed by rotation (see inset, Fig. 6), the peak current at higher light intensity clearly decreases as the rotation rate is increased.

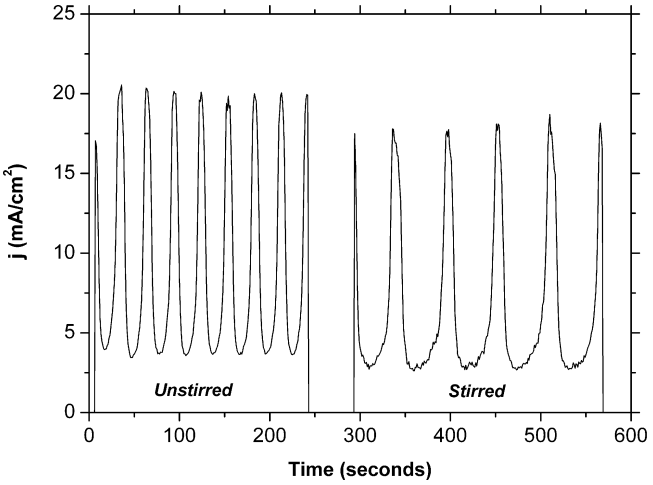

Fig. 5. Influence of hydrodynamics on the current oscillations. The mass transport was enhanced by stirring of a 0.1 M KOH solution.

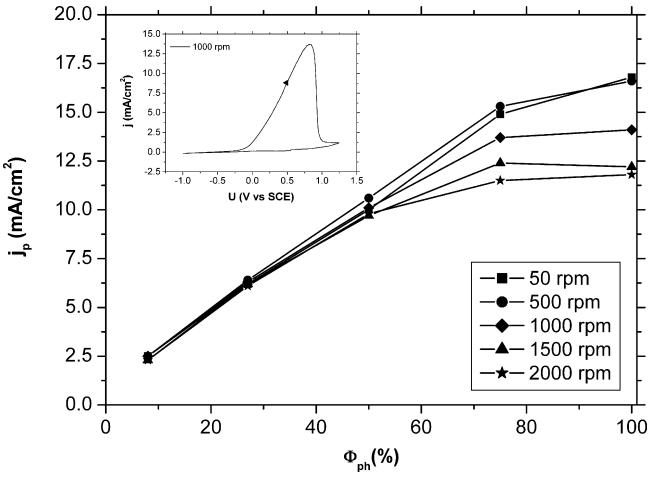

Fig. 6. Peak current as a function of light intensity for different rotation rates in 0.1 M KOH solution. The inset shows a cyclic voltammogram recorded at 1000 rpm at $\Phi_{ph} = 75\%$.

The charge passed during etching was measured and the etch depth was subsequently determined by profilometry. This allowed us to calculate the dissolution valence, i.e., the number of charge carriers required to etch 1 formula unit of SiC. In the active (pre-peak) range at 0.3 V, at the peak potential (0.5 V) and under conditions of sustained oscillation (0.65 V), values were found which varied between 6 and 6.8. The etch rate at the highest light intensity amounted to 350 nm/min. Etching in the active range (at 0.3 V) and in the range of sustained oscillations (at 0.65 V) gave a mirror-like surface; the root-mean-square roughness evaluated within a 25 μm^2 area using AFM was 38 and 22 nm, respectively. These values are considerably larger than the RMS roughness of the as-received (non-etched wafer), which was approximately 1 nm. Etching at the peak potential gave a matt surface and a surface roughness too large to measure reliably. The surface roughness found in this study is similar to that reported for galvanostatic experiments of Kato et al. [16].

4. Discussion

The dissolution valence of about 6 shows that the photoelectrochemical reaction of SiC in KOH solution must be exclusively the oxidation of the semiconductor; oxidation of water to give oxygen is clearly not important. Since Si is expected to be oxidized to a Si(IV) product, C very likely forms CO (with perhaps some CO_2). In the active dissolution range, the reaction occurring can be represented by

$$SiC + 8OH^- + 6h^+ \rightarrow [Si(OH)_2O_2]^{2-} + CO + 3H_2O \quad (1)$$

The silicate product dissolves in solution. High etch rates (up to 350 nm/min) are possible and the surface finish depends on the etching conditions.

At higher light intensity SiC passivates beyond a certain photocurrent density. This is due to the formation of a sparingly soluble oxide. The slow rate of oxide dissolution can explain the hysteresis in the cyclic voltammograms. These voltammetric features are reminiscent of the electrochemistry of Si in KOH solution, shown for comparison in Fig. 7. At a scan rate of 10 mV/s both p- and n-type Si(100) give a similar active/passive transition in 0.1 M KOH solution.

There are, however, some striking differences between Si and SiC: (i) the current density required to achieve passivation is much lower for Si than for SiC. At the highest light intensity shown in Fig. 2 for 0.1 M KOH solution this difference is more than a factor of 200; (ii) the hysteresis observed for Si is significantly larger than for SiC; oxide removal is observed only at very low scan rates in the reversed scan direction for Si(100); (iii) while the critical current density for the passivation of Si depends only on the KOH concentration (it is the same for n- and p-type electrodes [21]), the peak current density for SiC clearly depends on the light intensity (see Fig. 2). In contrast, for the case of photoanodic oxidation of n-type Si in acidic

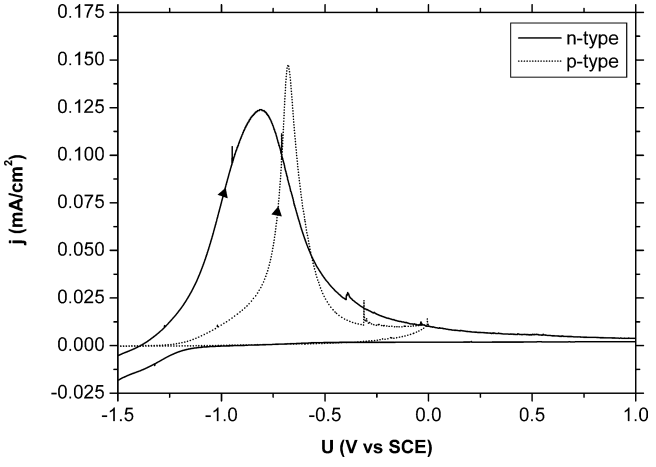

Fig. 7. Current density–potential plots of n-type (solid line) and p-type Si(100) (dotted line) in the dark in 0.1 M KOH solution.

fluoride solution there is a limiting light intensity for the formation of oxide. Above this light intensity the photocurrent-potential curve is independent of the photon flux; (iv) the effect of enhanced mass transport is surprizing: the current density decreases with solution stirring or an increase in rotation rate of an RDE. Such effects are not observed with Si.

At potentials below the peak value the reaction products, silicate species and CO, are efficiently removed from the electrode surface. That this can occur to current densities much higher than for Si without passivation occurring is very likely due to the presence of carbon in the crystal matrix and its conversion to CO at a surface lattice site; this will hinder the formation of a coherent silicon oxide network. This raises the question as to why the surface finally passivates; oxygen in solution does not play a role. Since passivation occurs at a current density dependent on the light intensity, a precipitation of oxide from dissolved silicate species is unlikely. The results shown in Fig. 6 (the peak current decreases with increasing rotation rate) confirms this conclusion. The limiting photocurrent at low light intensity and the peak current at high intensity are directly proportional to the photon flux (Figs. 1 and 2). These results show that the rate of photoanodic oxidation is determined mainly by the hole flux to the surface. Oxide formation occurs only when a critical photocurrent is reached, which depends on light intensity. Passivation requires the nucleation of surface oxide, which could be facilitated by adsorption of the silicate anions at the surface. This would suggest that surface charging of the electrode might be important. A limiting photocurrent is observed when electron-hole recombination is suppressed by the strong electric field of the space charge layer. Surface recombination is very likely the more dominant mechanism. If recombination occurs by hole trapping at the surface followed by electron capture, then the concentration of positively charged traps will increase as the electron concentration decreases, i.e., as the electrode potential is made more positive. At the same time the photocurrent (the competing reaction) increases. A limiting photocurrent is obtained when all the traps are occupied. We speculate that the build-up of positive charge localized in surface traps could lead to chemisorption of negatively charged silicate species and the initiation of oxide growth

$$[\mathrm{Si(OH)_2O_2}]^{2-}_{\mathrm{ads}} + (n-1)[\mathrm{Si(OH)_2O_2}]^{2-} \rightarrow n\mathrm{SiO_2} + 2n\mathrm{OH^-} \quad (2)$$

In view of the results shown in the inset of Fig. 2 this hypothesis implies that the photocurrent density corresponding to the critical surface charge (i.e., that initiating passivation) depends linearly on the light intensity. A simple kinetic model predicts that the fraction of occupied surface states is determined by the photocurrent density normalized with respect to the photon flux [22].

The fact that improved hydrodynamics lowers the limiting photocurrent must mean that transport of a solution species to the surface or of a product from the surface slows down the electrochemical reaction. Our results show that dissolved oxygen is not responsible for the effect. It is difficult to see how mass transport of silicate or OH^- ions could explain the result (see Eq. (1)). On the other hand, the removal of CO from surface sites allows the interlinkage of silicate species and thus partial or complete blockage of the surface. In this way, the mass transport limited removal of large quantities of CO produced could determine the surface coverage by oxide and thus the kinetics of the reaction.

Two aspects of the photoanodic etching of SiC in KOH solutions are interesting for device technology. In the onset of the photocurrent, where electron-hole recombination is important, our work and that of others [16–18] shows that etching is defect selective. At more positive potentials high etch rates (up to 350 nm/min) are achieved. The surface roughness of the etched wafers reported here is, however too high. Our preliminary results with experiments at higher temperature ensuring higher oxide dissolution rates suggests that electropolishing of SiC may be possible in alkaline solution.

Acknowledgements

The authors thank Umicore for providing the 4H -SiC wafers and Jan Weyher (Radboud University Nijmegen, The Netherlands) and Harold Philipsen for contributing to this work. This work was financially supported by the Dutch Technology Foundation (STW, UPC-6317).

References

[1] G.L. Harris (Ed.), Properties of Silicon Carbide, INSPEC, London, 1995.
[2] M. Katsuno, N. Ohtani, J. Takahashi, H. Yashiro, M. Kanaya, Jpn. J. Appl. Phys. 38 (1999) 4661–4665.
[3] A.J. Rosenbloom, Y. Shishkin, D.M. Sipe, Y. Ke, R.P. Devaty, W.J. Choyke, Mater. Sci. Forum 457–460 (2004) 1463–1466.
[4] A.J. Rosenbloom, D.M. Sipe, Y. Shishkin, Y. Ke, R.P. Devaty, W.J. Choyke, Biomed. Dev. 6 (2004) 261–267.
[5] Y. Shishkin, W.J. Choyke, R.P. Devaty, J. Appl. Phys. 96 (2004) 2311–2322.
[6] P.H.L. Notten, J.E.A.M. van den Meerakker, J.J. Kelly, Etching of III–V Semiconductors, Elsevier Advanced Technology, 1991.
[7] J.S. Shor, I. Grimberg, B.Z. Weiss, A.D. Kurtz, Appl. Phys. Lett. 62 (1993) 2836–2838.
[8] J.S. Shor, R.M. Osgood, J. Electrochem. Soc. 140 (1993) L123–L125.
[9] J.S. Shor, A.D. Kurtz, J. Electrochem. Soc. 141 (1994) 778–781.
[10] J.S. Shor, X.G. Zhang, R.M. Osgood, J. Electrochem. Soc. 139 (1992) 1213–1216.
[11] X.G. Zhang, S.D. Collins, R.L. Smith, J. Electrochem. Soc. 136 (1989) 1561–1565.
[12] R.L. Smith, S.D. Collins, J. Appl. Phys. 71 (1992) R1–R22.
[13] H.G.G. Philipsen, J.J. Kelly, J. Phys. Chem. B 109 (2005) 17245–17253.
[14] X.H. Xia, C.M.A. Ashruf, P.J. French, J. Rappich, J.J. Kelly, J. Phys. Chem. B 105 (2001) 5722–5729.
[15] P. Raisch, W. Haiss, R.J. Nichols, D.J. Schiffrin, J. Phys. Chem. B 105 (2001) 12508–12515.

[16] M. Kato, M. Ichimura, E. Arai, P. Ramasamy, Jpn. J. Appl. Phys. 42 (2003) 4233–4236.
[17] M. Kato, M. Ichimura, E. Arai, P. Ramasamy, J. Electrochem. Soc. 150 (2003) C208–C211.
[18] J.L. Weyher, S. Lazar, J. Borysiuk, J. Pernot, Phys. Stat. Sol. 202 (2005) 578–583.
[19] J. van de Lagemaat, D. Vanmaekelbergh, J.J. Kelly, J. Appl. Phys. 83 (1998) 6089–6095.
[20] O.J. Glembocki, E. Stahlbush, M. Tomkiewicz, J. Electrochem. Soc. 132 (1985) 145.
[21] The mechanism of current generation for Si is quite different from that of SiC. However, passivation is caused in both cases by the passage of anodic current.
[22] J.J. Kelly, R. Memming, J. Electrochem. Soc. 129 (1982) 730–738.